

4 A New Microscopic Technique for Quantitative Analysis of Paper Structure at the Fibre Level

4.1 Introduction

Chapter 2 has reviewed how researchers have attempted to describe the strength properties of paper in terms of the structural properties of the fibre network and the mechanical properties of the fibres (Cox 1952; Page 1969; Kallmes 1977). Fibre dimensions and 3-dimensional orientation have been shown to be very important for paper strength in these studies. However, no technique is available to obtain quantitative data of fibre dimensions and this 3-dimensional orientation in situ to fully verify these network models. In recent studies on the paper mechanics, it has also been shown that better understanding of the structure of paper at the fibre level is required. This project starts from analysis of paper structure as the basis for development of a new model for the tensile strength of paper.

It is essential to expose and image the internal structure of paper for structure analysis and many techniques have been used for doing this. The most commonly used technique to expose internal structure is thin sectioning (microtomy). Some examples of the successful use of thin sectioning to study paper structure, using both transmitted light and electron microscopy are given in references (Page 1965; Quackenbush 1971; Nanko 1989; Szikla 1989). The main problem of thin sectioning is that the sample structure can be distorted during mechanical sectioning. Its use for quantitative analysis of paper structure is therefore problematical.

Williams et al (Williams 1994) and Williams and Drummond (Williams 2000) recently developed a new technique in which samples were embedded in resin and the cross-sections of the samples were then exposed by grinding the block surface using progressively finer abrasive papers. In order to get proper topographic contrast for scanning electron microscope (SEM) viewing, chemicals were used to etch away a layer of the supporting resin from the block surface. The Williams et al technique avoids exposing the sample to the compressive and shear forces developed during the thin sectioning. However, great care must be taken during surface resin removal with

chemicals to avoid swelling of the exposed fibres and paper surface. In addition to this, the SEM can only obtain the image of the cross-sectional surface, and this may not be free of artifacts of sample preparation. Using this technique, Forseth and Helle (Forseth 1997) quantified the change in fibre lumen area in paper during moistening. In their study, only fibres cut more or less parallel to the fibre length direction were measured to prevent overestimation of the fibre wall thickness.

Confocal laser scanning microscopy has been commonly used in qualitative analysis of paper structure in recent years (Li 1997; Moss 1997; Ting 1997). The major feature of the CLSM is its optical sectioning capability, which can be used to obtain three-dimensional images of fibre and paper non-destructively. However, the signal intensity diminishes rapidly with increasing depth in the sample (Li 1999). Therefore these studies, which looked through the in-plane surface of the samples, could not obtain a complete view of a sheet cross-section. (Li 1997; Moss 1997; Ting 1997).

More recently, Dickson (Dickson 2000a; Dickson 2000b) conducted successful quantitative analysis of paper cross-sections using a combination of the sample preparation technique developed by Williams and Drummond (Williams 2000) and the confocal laser scanning microscopy technique. Complete cross-sections of paper were imaged with CLSM just below the cross-sectional surface to avoid the artifacts on the surface (Dickson 2000a). Dickson quantified the profile properties of the paper cross-section including the wall area, the total pore area, interfibre pore area and lumen area. The dimensions of individual fibres in the sheet were not measured in any of these studies.

Fibre orientation has often been measured by tracing a fraction of dyed fibres in a sheet (Perkins 1981; Rigdahl 1983). The fibre orientation measured by this technique is the in-plane orientation and the fibres traced are always limited to the paper surface. Another technique is to split a sheet into thin, transparent layers and then measure the fibre orientation with image analysis in all these layers (Erikkila 1998). This technique allows the in-plane fibre orientation in different layers to be measured but not the out-of-plane fibre orientation. A more accurate and relatively easy technique is still required for measurement of overall fibre orientation.

In this chapter, we present a new method for quantifying paper structure. The dimensions and orientations of individual fibres in a sheet are measured simultaneously using a combination of resin embedding and confocal laser scanning microscopy. This is the first technique that can simultaneously obtain all this information directly in situ. Based on this technique, we further developed a technique for measuring the properties of fibre-fibre contacts including the nature of fibre contact, the number of fibre-fibre contacts, the length of free fibre segment and the out-of-plane angle of each free fibre segment. This work is presented in Chapter 7. This is also the first technique that can simultaneously measure all these quantities directly in paper.

4.2 Basic idea of the new technique

The basic idea of this new technique is to examine the individual fibres in paper directly by using a confocal microscope. Paper samples were arranged vertically and embedded in resin. The sample cross-section was exposed by grinding the resin block with abrasive paper. It is critically important that the sample is thoroughly penetrated by the resin to provide sufficient support to the paper structure. Once quality images of the paper cross-section was obtained, measurement of fibre dimensions, fibre orientation and fibre-fibre contacts was carried out in these images by using different macros written in the commercial software package Optimas 6.1.

4.3 Experimental equipment and methods

4.3.1 Confocal microscope

A confocal laser scanning microscope (CLSM) was used to measure the cross-sectional dimensions of fibres on glass slides and in paper. The CLSM used in this project was the Optiscan F900e that was fitted to an Olympus BH2 optical microscope. The CLSM can operate in either reflectance or fluorescence mode. In reflectance mode the image is the light that has been reflected from the sample while in fluorescence mode, fluorescence excited by the incident laser beam is detected. To use the fluorescence

mode, the sample must either be naturally fluorescent or fluorescent dye must be added. This mode was used for all of the confocal work presented in this thesis.

The Optiscan F900e uses an optic fibre to deliver the laser light through the optic system of the microscope and to collect the light signal from the excited fluorescent dye contained in the fibres.

Figure 4-1 schematically shows the principle of the confocal microscope. The laser used was an Argon-Ion laser operating at a wavelength of 480nm. The signal from the excited fluorescent dye is passed back through the optical path and through a small aperture, the confocal pinhole, before reaching an electronic detector or photo-multiplier tube (PMT). The PMT converts the light into a digital image displayed on a computer monitor. Because of the confocal pinhole, only light returning from on or very near the focal plane is permitted to pass through to the PMT. Light returning from other than the specific optical plane is blocked. This process creates an extremely thin optical section that can be positioned within a specimen to potentially provide a sharp image with a significantly higher resolution than a conventional microscope.

For optimum performance in the confocal microscopy, it is necessary to keep to a minimum, the degree of refractive index mismatch between the object being investigated and its surrounding medium. If there is a large refractive index mismatch between the fibres then the refraction of light from irregular surfaces in the object will cause lower levels of signal to be sent back to the PMT, something that will affect the image quality. This will be compounded when attempting to obtain images below the sample surface (scanning inside the sample). Therefore, full saturation of the fibre samples with oil of similar refractive index (RI) and removal of the air trapped in the fibres are essential for obtaining quality images. The immersion oil used had an RI of 1.51. It was specially designed for oil objective lenses.

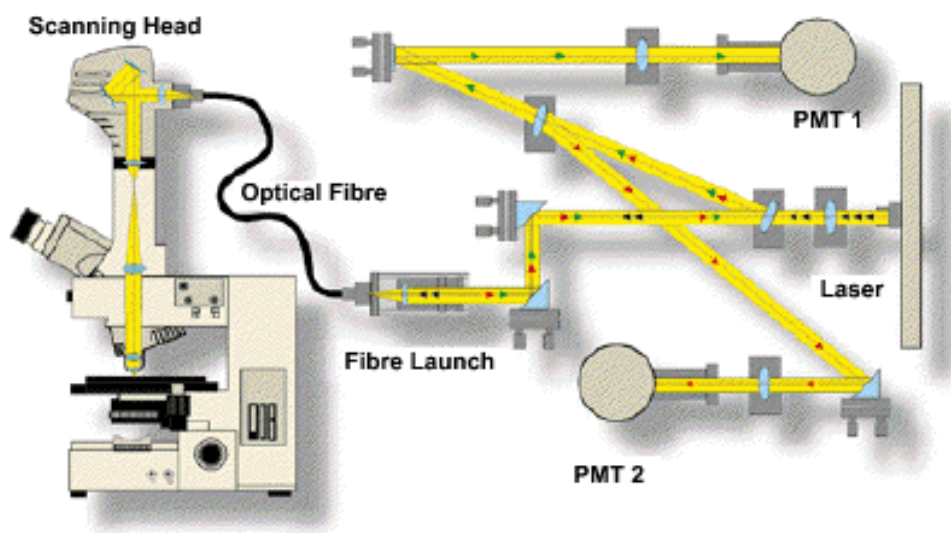


Figure 4-1 Schematic showing the basic principle of the optical system of the Optiscan F900e system (From Optiscan Pty Ltd)

4.3.2 Sample preparation

Recycled pulp of commercial plaster line board and laboratory made never dried radiata pine kraft pulp (kappa no. 95) (refer to Appendix A for details of these pulp) were used in the experiments for development and validation of the new technique.

4.3.2.1 Staining of pulp fibres and handsheet formation

The fibres were stained in a stock divider at a consistency of 1.5 % prior to handsheet formation. The dye (Acridine Orange) was added at a rate of 0.0005% w/w water. From each pulp, three sets of square handsheets were made on a Moving Belt Sheet Former (Xu and Parker 2000). Each set of the handsheets from each pulp were pressed dynamically using the Sheet Roll Press at one of three pressing levels, viz P_1 , P_2 and P_3 (see Subsection 5.2.1). The handsheets made from the recycled pulp were denoted as R_0 , R_L and R_H , and those made from the kraft pulp were denoted correspondingly as Kp_0 , Kp_L and Kp_H .

4.3.2.2 Sample embedding – Initial technique

The sample embedding technique presented in this subsection was used only at the beginning of the project when the new microscopic technique was verified. It was found that it could be improved during verification of the new technique. The improved technique will be discussed in the next subsection.

The resin used for sample embedding was Epofix (from **(Struers)**). This resin met the following criteria:

- a. no reaction with fibres
- b. good penetration into the fibres
- c. refractive index of the resin block is 1.57, which is close to the fibre refractive index 1.53.

Samples were first placed directly in 100% resin and degassed overnight so that the resin could penetrate into the paper structure and expel gas in the paper. The samples were then taken out of the resin and put on a plate for about 5 minutes to allow the resin at the sample surfaces to drain away. The samples were then put into a plastic mould, and a pre-degassed mixture of resin and hardener (15 parts of resin and 2 parts of hardener) was poured into the mould and the whole sample was put into a vacuum apparatus and left until the resin cured into block. It is very important to ensure that all gas is removed from the samples and the internal structure of the paper is thoroughly penetrated by the mixture of resin and hardener. The cross-sections of the samples were then exposed by abrading the block surface with a range of abrasive papers of decreasing roughness (P400, P600, P800 P1200, P1500 and P2400). Figure 4-2 shows an embedded sample ready for examination in the confocal microscope.

4.3.2.3 Sample embedding – improved technique

As will be discussed later in this chapter, the embedding technique outlined in the above subsection may not provide a thorough penetration of the resin and hardener mixture into the sample structure. A new rig, a vacuum impregnation apparatus, as illustrated in

Figure 4-3, was designed and used to improve the sample embedding technique. The improved technique was used in the subsequent experimental work.



Figure 4-2 Embedded sample ready for examination in confocal microscope

The pre-cut sample was vertically put into the mould. The sample and the mould were then put into the container. Valve 2 is closed and valve 1 is opened. The vacuum is applied for at least for 4 hours to first remove air trapped in the sample structure. Then valve 1 is closed and valve 2 is opened to suck the resin and hardener mixture into the mould. A vacuum impregnation is created with this procedure, which can provide a thorough penetration of the mixture into the sample structure. When enough resin mixture has been sucked into the mould, valve 2 is closed and valve 1 is opened to apply vacuum to the whole system for at least another 4 hours to further remove air in the sample and the resin mixture.

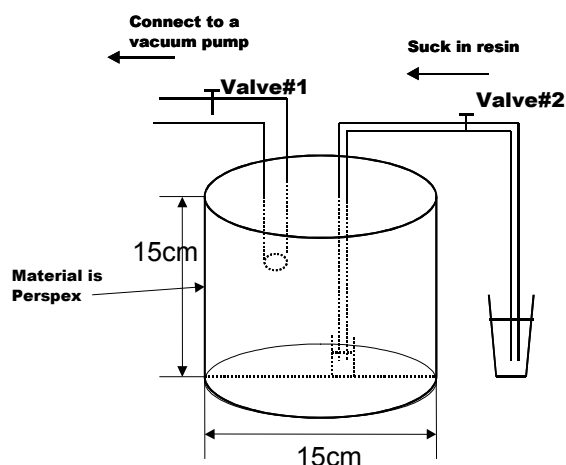


Figure 4-3 Schematic drawing of the vacuum impregnation apparatus

4.4 Quantitative analysis of paper structure

4.4.1 Measurements of fibre orientation and shape

4.4.1.1 Imaging and image analysis

Imaging was performed with the Optiscan C900e confocal laser scanning microscope using a 60 \times oil immersion lens (see Figure 4-4). The inspection area of each image frame was 100 \times 100 μ m with a resolution of 512 \times 512 pixels.

For each region of interest, a group of images of the region was captured at different depths from the cross-sectional surface. Fifty groups of cross-sectional images of each sample were captured and processed for measurement of fibre orientation and fibre cross-sectional dimensions. A typical group of cross-sectional images of the paper is given in Figure 4-5. The images shown in Figure 4-5 were obtained using the initial embedding technique as discussed in subsection 4.3.2.2. The data used for verification of the new technique in this chapter were measured in images of samples embedded using the initial embedding technique. In the rest of the project, the improved embedding technique was used for sample preparation. The image with 0-depth was

captured just below the exposed surface of the sample. The depths of the other images are measured with respect to the 0-depth image. It can be seen that the image brightness decreases with increasing depth. The maximum scanning depth used in this study was 10 μ m. Scanning deeper led to a rapid deterioration of image quality.

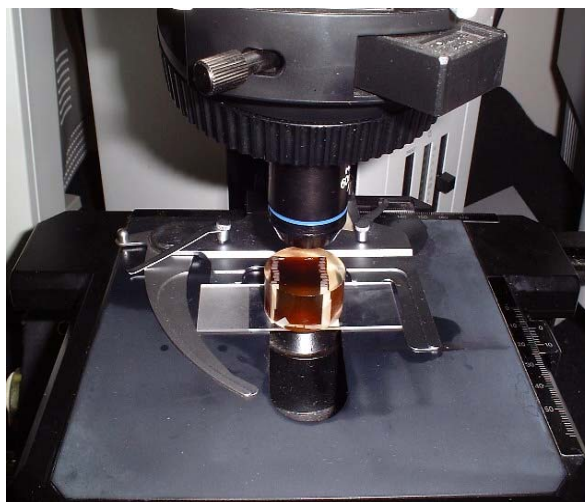
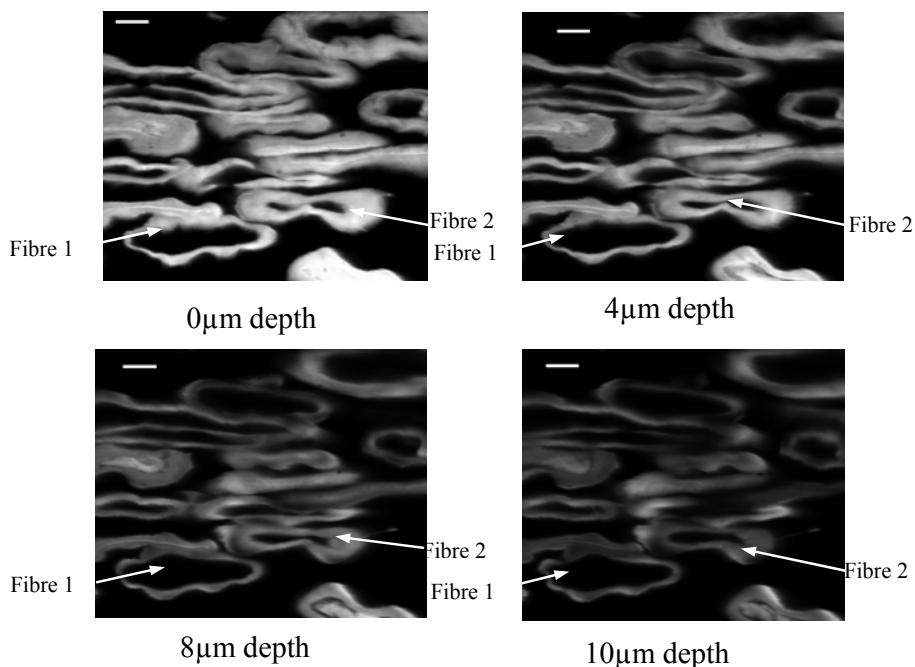


Figure 4-4 Picture showing a sample on the stage of a confocal microscope



**the scale bar is 10 μ m*

Figure 4-5 Cross-sectional images of paper acquired at depth of 0, 4, 8 and 10 μ m (for the explanation of the depth see text).

The image analysis was conducted using the commercial image analysis software (OPTIMAS 6.1). The analysis sequence used was: 1) select a region of interest; 2) smooth the image with a 3×3 Gaussian filter; 3) adjust the threshold level; and 4) extract features including fibre wall area, mass centre of fibre cross-sectional area, fibre width (D_w) and fibre height (D_h). A macro was written in the software for performing the above process automatically (see Appendix D). The boundary of a fibre was identified by manually adjusting the threshold. For those fibres that touched each other, a line was drawn between them to separate the fibres but keep the features of the fibre of interest unchanged. The following subsections discuss the quantities of paper structure were measured directly in the paper cross-section by using the new microscopic technique. Some of the quantities are defined for the first time in this project.

4.4.1.2 Fibre orientation

Fibre orientation was measured by following the positions of individual fibres in sheet cross-sections scanned at 0 μ m depth and 10 μ m depth. The position of the mass centre of the fibre cross-section was determined by the distance from the mass centre to a reference point in the Y and Z directions. As shown in Figure 4.6, the mass centre of the fibre cross-section in the 0-depth image is (Y_1, Z_1), and in the 10 μ m depth image is (Y_2, Z_2). The angle θ that the fibre makes to the X direction (the plane of the paper) can then be calculated from geometry. For example, in Figure 4-5, the position of fibre 1 has no apparent change when scanning down from 0-depth inside the sample to 10 μ m deep. This indicates fibre 1 is almost perpendicular to the exposed surface. However, the position of fibre 2 shifts markedly indicating that fibre 2 sits at an angle other than 90° to the exposed surface of the sample.

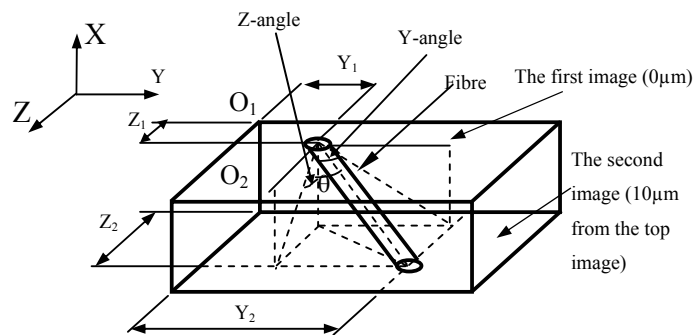


Figure 4-6 Depiction of Measurement of fibre orientation in paper.

4.4.1.3 Fibre in and out of plane angle

The fibre orientation angle, θ , measured by using the above method is the overall angle. As shown in Figure 4-6, if needed the out of plane angle (the Z-angle), and the in-plane angle (the Y-angle) can also be calculated from geometry.

4.4.1.4 Fibre wall area

For the work in this Chapter, the wall areas of fibres from both pulps were measured from both the 0 μm and 4 μm depth images. In the rest of the project, when the improved sample embedding technique was used, the fibre dimensions were measured in images acquired just below the sample surface. If the fibre is not perpendicular to the paper cross-section, the wall area will be enlarged by a factor of $1/\cos\theta$. The measured wall area of each individual fibre has been corrected by this factor.

The fibre wall areas of the two pulps were also measured on freely dried fibres on glass slides using the confocal laser scanning microscope following a procedure described by (Xu, Conn et al. 1998). Details of sample preparation and image analysis for this measurement is given in Appendix B. These results were compared with the fibre wall areas measured in situ on fibres in paper sheets for the purpose of verification of the new technique.

4.4.1.5 Fill factor, Shape factor and twist angle

As discussed in Chapter 3, the fill factor is defined for the purpose of modelling the structure of paper. The fill factor, f_h , is defined as the ratio of the fibre wall area, A_f , to the area of the smallest rectangle bounding box, A_{bf} , that can completely enclose the irregular shape of the fibre and with its one side parallel to the paper plane (see Figure 3-3). The fill factor was calculated by the measured fibre wall area divided by the area of the rectangular bonding box for each individual fibre. The rectangular bonding box was generated automatically by running the macro (refer to Appendix D).

In order to quantify the degree of fibre collapse, an additional shape factor is defined. As shown in Figure 4-7, the shape factor, f_m , is defined as the ratio of the fibre wall area, A_f , to the area of the smallest rectangular bounding box, A_{bm} , that can completely enclose the irregular shape of the fibre. The two axes of the rectangular box are then defined as the major and minor axes of the fibre cross-section. When the fibre is in a cross-section of paper, the angle between the major axis of the fibre and the paper plane is defined as the twist angle of the fibre cross-section.

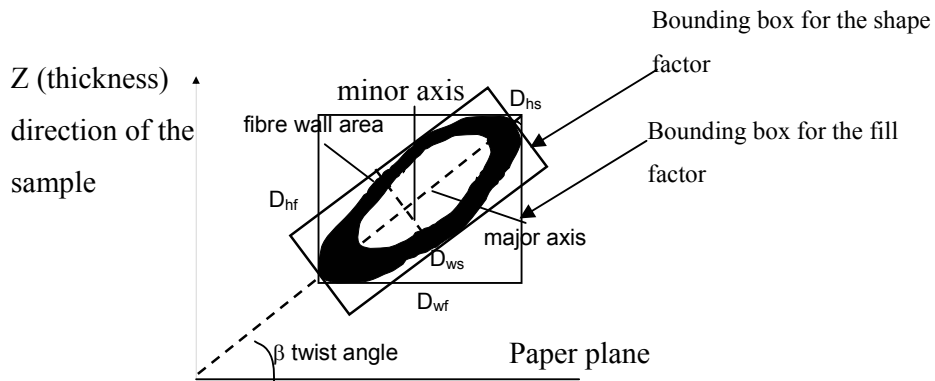


Figure 4-7 Definition of the fibre shape factor and twist angle

In order to measure f_m and the twist angle, β , we need firstly to create the smallest rectangle that encloses the irregular shape of the fibre. In practice, it is difficult to calculate this smallest rectangle. The bounding box used in this study was a rectangle with its major axis parallel and equal in length to the longest dimension of the fibre cross-section. For most types of fibre shape this bounding box is very similar to the

smallest rectangle in the definition of f_m . The measurement error is significant only for square shaped fibres. However, the square shaped fibres were rare in the pulp used in this study and were discarded during measurement. The percentage of the fibres been discarded for the particular samples will be given in Chapter 6.

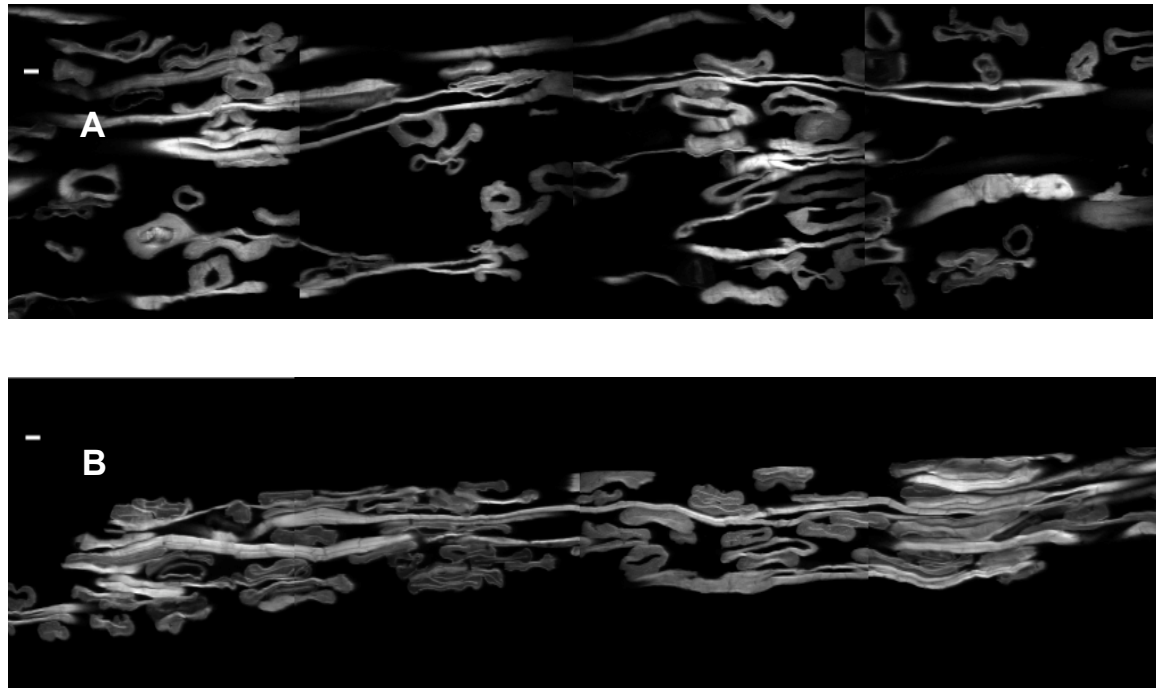
The twist angle used was the measured angle between the longest dimension of the fibre cross-section and the horizontal frame of the image. This reference direction has to be used because the position of the paper plane is unknown during the measurement. However, if the horizontal frame of the image is at an angle $-\alpha$ to the paper plane, then it can be shown that, for a randomly oriented handsheet, $\bar{\beta} = \alpha$. We estimated the angle α by averaging the measured twist angles. The twist angle was also corrected by the angle, θ , that the fibre is sitting to the surface of the paper cross-section. If the fibre length axis is not perpendicular to the paper cross-section, then one axis of the fibre image will be lengthened by a factor of $1/\cos\theta$. Thus unless $\beta = 0$, this distortion of one axis will cause an error in the measured value of β . It can be shown from geometry that the true angle β is given by $\beta = \arcsin\left(\frac{\sin\beta_m}{\cos\theta}\right)$, where β_m is the measured twist angle. All measured twist angles were first corrected by the angle α and then by the angle θ using the above formula.

4.4.2 Measurement of fibre-fibre contacts

The measured parameters associated with the fibre-fibre contacts included the nature of fibre contact, the number of fibre-fibre contacts, the lengths of the free fibre segments and the out-of-plane angle of each free fibre segment. These parameters were measured directly in images of paper cross-sections. For each sample, 70 frames of cross-sectional images were obtained consecutively along the sample cross-section using the confocal laser-scanning microscope and the 60x oil-immersion lens. The inspection area of each image was $200 \times 200 \mu\text{m}^2$, and the resolution was 512×512 pixels. The 70 images were then joined together in consecutive order during the measurements, therefore a 14mm length of the sample cross-section was imaged in this way. Some fibres or fibre segments in the sample cross-section were imaged along their long axes.

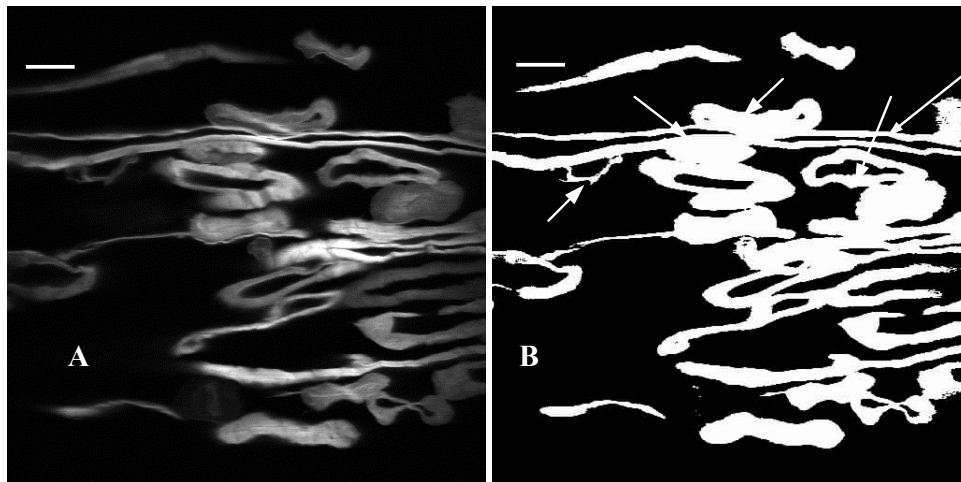
These fibres were chosen as the fibre of interest for the measurements of fibre-fibre contacts. Two images of such fibres are shown in Figure 4-8. When such a fibre was chosen, the number of fibres in contact with the fibre of interest was counted, and a line was drawn between the centres of two neighbouring contacts along the fibre axis. The length of the line is the free fibre length and the angle between the line and the horizontal frame of the image is the measured out-of-plane angle of the free fibre segment. If the horizontal frame of the image is at an angle $-\alpha$ to the paper plane, then it can be shown that, for a randomly oriented handsheet, the average value of the out-of-plane angles of all the free fibre segments in the paper is equal to α . We estimated the angle α by averaging the measured out-of-plane angles and we then corrected all the measured out-of-plane angles by the angle α .

To identify fibre-fibre contacts, the cross-sectional images of the samples were first thresholded manually, and then binaried into black and white images. In the binary images, fibre-fibre contacts could easily be identified. If there is no black gap between two fibre surfaces, we defined that a contact has been made between these two fibres. Otherwise, there is no contact between them. In this project, fibre-fibre contacts were classified into full contacts and partial contacts. The cross-section of a fibre is assumed to have two long sides and two short sides. When one of the long sides is totally in contact with the fibre of interest, this contact is a full contact. Otherwise, the contact is a partial contact (see Figure 4-9). All these image analysis and measurements were conducted using the Optimas 6.1 software.



* the size bar is 10 μ m

Figure 4-8 Images of paper cross-sections (A is sample Rej-P₀ and B is Rej-P_H)



* the size bar is 20 μ m

Figure 4-9 Cross-section image before (A) and after (B) thresholding and binarisation. Fibre 2 and 3 in (B) make two full contacts, fibre 1 makes a partial contact, and fibre 4 is not in contact with the fibre of interest.

The measured results of fibre-fibre contacts will be discussed in detail in Chapter 7.

4.5 Validation of the new technique

The new technique for microscopic analysis of paper structure was validated by comparing the fibre dimensions measured by the new technique in paper with those measured on fibres dried on slides by the route confocal microscopy method. The validity of the new technique was further checked by comparing the measured fibre orientation with the theoretical value of a random sheet.

4.5.1 Comparison of the fibre wall area measured in paper with that measured on slide

Table 4-1 summarizes the fibre dimensions and the sheet properties measured in this study. As can be seen from Table 4-1, the average fibre wall areas of the recycled pulp samples R_0 , R_L and R_H are very close to each other, especially for those measurements acquired $4\mu\text{m}$ below the sample surface. A similar situation is shown for the kraft pulp samples Kp_0 , Kp_L and Kp_H . This is as expected because wet pressing should not change the wall areas of fibres in the sheets.

Table 4-1 A summary of the experimental results

| Pulp Sample | Handsheet Sample Code | Apparent density (kg/m ³) | Tensile index (kNm/kg) | Fibre wall area (μm ²) (at 0μm depth) | Fibre wall area (μm ²) (at 4μm depth) | Fill factor (at cross-sectional surface) | Fill factor (at 4 μm depth) | Fibre angle to X-direction (degree) | Number of fibre measured |
|--------------------------------------|-----------------------|---------------------------------------|------------------------|---|---|--|-----------------------------|-------------------------------------|--------------------------|
| Recycled pulp | R_0 | 234 | 17.3 | 220±9* | 181±9* | 0.56±0.01 | 0.54±0.01 | 25.8 | 147 |
| | R_L | 334 | 22.9 | 223±9 | 179±9 | 0.53±0.01 | 0.55±0.01 | 24.6 | 146 |
| | R_H | 380 | 22.3 | 209±10 | 172±9 | 0.56±0.01 | 0.57±0.01 | 26.0 | 147 |
| Recycled pulp fibres dried on slides | / | / | / | 170±8 | 170±8 | / | / | / | 319 |
| Kraft pulp | Kp_0 | 112 | 13.1 | 312±9 | 266±9 | 0.45±0.01 | 0.46±0.01 | 28.1 | 176 |
| | Kp_L | 215 | 29.2 | 295±10 | 256±9 | 0.50±0.01 | 0.48±0.01 | 25.2 | 192 |
| | Kp_H | 393 | 51.0 | 294±10 | 260±9 | 0.55±0.01 | 0.56±0.01 | 26.9 | 180 |
| Kraft pulp fibres dried on slides | / | / | / | 249±9 | 249±9 | / | / | / | 338 |

* ± is 95% confidence interval.

Comparisons were made between the fibre wall areas measured in sheets and those measured on dried fibres on glass slides for the purpose of validating the measurements of the new method. As shown in Table 4-1, for both of the pulps used in this study, when the fibre wall areas were measured in images of paper cross-sections scanned $4\mu\text{m}$ below the sample surface, the results are very close to those measured on the same pulp fibres dried on glass slides. The maximum difference between them is $11\mu\text{m}^2$ for the recycled fibres and $17\mu\text{m}^2$ for the kraft fibres. The frequency distributions of fibre wall areas of these measurements are given in Figure 4-10 for the recycled pulp and Figure 4-11 for the kraft pulp. From these figures, it can be seen that the distributions of fibre wall areas of samples made from the same pulp fibres but pressed at different pressing levels are not only in close agreement with each other but also in close agreement with those measured on the freely dried fibres on glass. The fibre wall areas of recycled fibres were mostly distributed between $100\mu\text{m}^2$ and $200\mu\text{m}^2$, and between $200\mu\text{m}^2$ and $350\mu\text{m}^2$ for the kraft fibres. These comparisons indicate that the measurements of fibre wall areas using the proposed new method and taking measurements from images of paper cross-sections acquired $4\mu\text{m}$ below the surface of the sample cross-sections are valid.

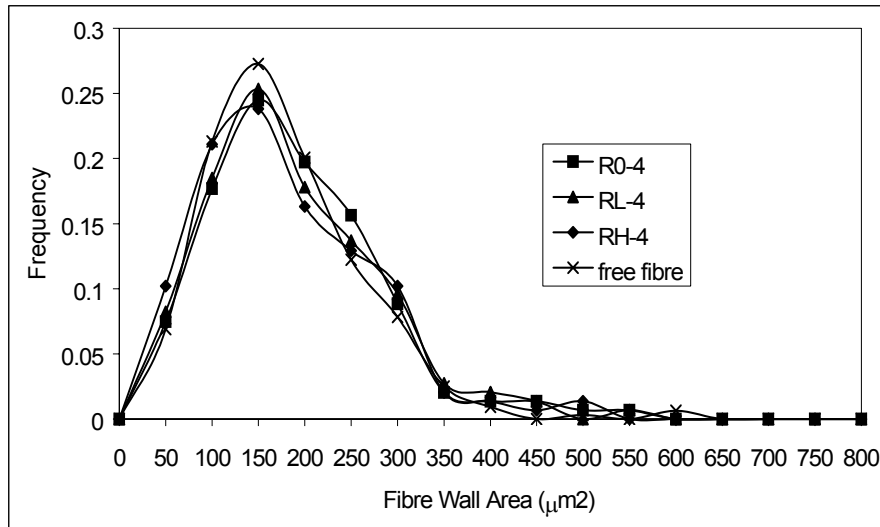


Figure 4-10 Distribution of fibre wall areas measured in paper and on slides for the recycled fibres. The fibre wall areas measured in paper were determined from images taken at $4\mu\text{m}$ depth.

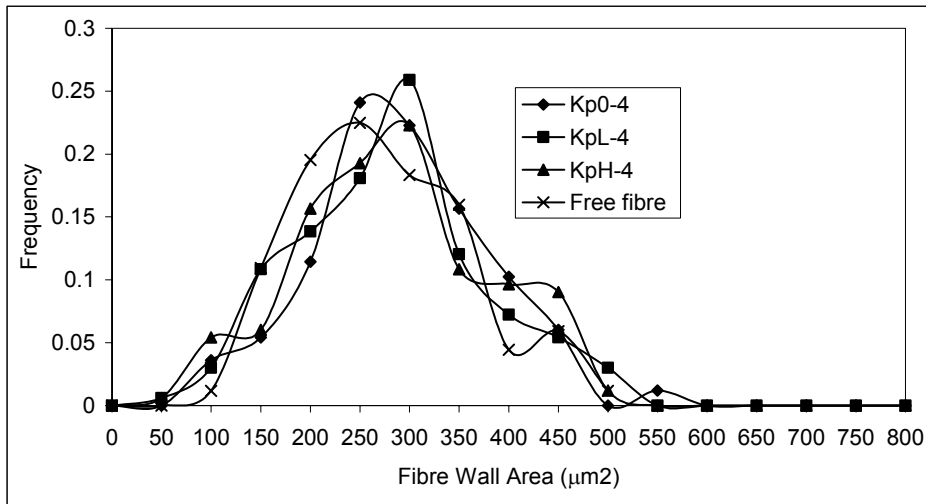


Figure 4-11 Distribution of fibre wall areas measured in the sheet and on slide for the kraft fibres. The fibre wall areas measured in paper were determined from images taken at 4µm depth.

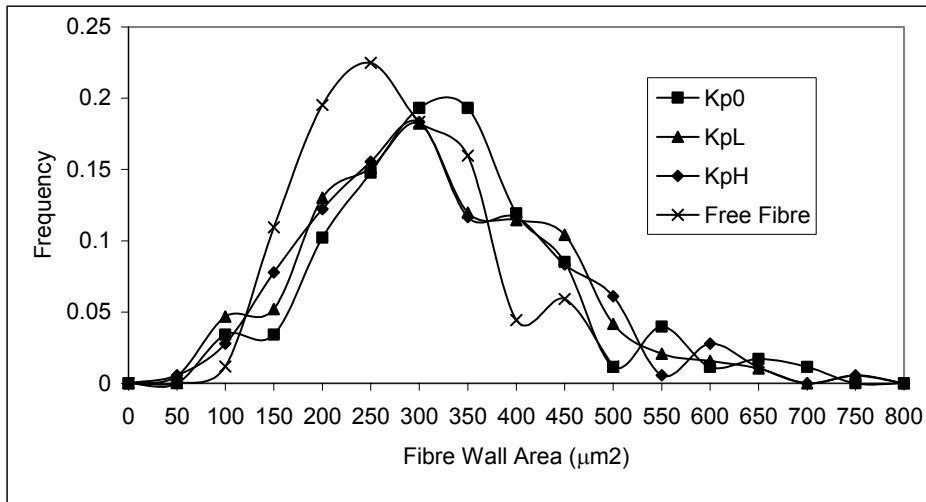


Figure 4-12 Distribution of fibre wall areas measured in the sheet and on slide for the kraft fibres. The fibre wall areas measured in paper were determined from the surface images.

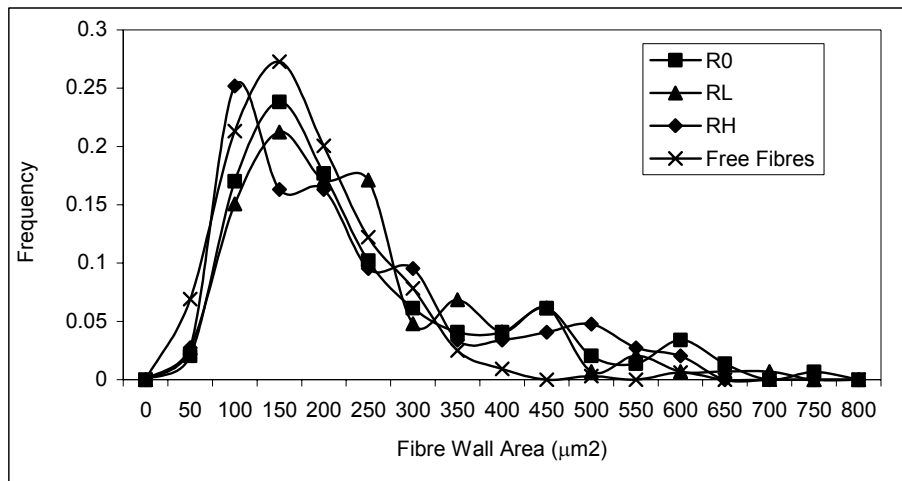


Figure 4-13 Distribution of fibre wall areas measured in the sheet and on slide for the recycled fibres. The fibre wall areas measured in paper were determined from the surface images.

When the measurements were made in the $0\mu\text{m}$ depth images of the paper cross-sections, the mean values of the fibre wall areas of both pulps are greater than those of their corresponding freely dried fibres (see Table 4-1). The average difference is $50.9\mu\text{m}^2$ for the kraft fibres and $47.2\mu\text{m}^2$ for the recycled fibres. Despite these relatively large differences in average fibre wall areas, the frequency distributions are still quite similar (see Figure 4-12 and Figure 4-13). It is very interesting to note that the results measured in sheets showed some large values (greater than $500\mu\text{m}^2$), which could not be seen in the results measured on free fibres from the same pulp. It is believed that these large fibre wall area values result from artifacts produced by sample preparation. A careful observation of the images of the paper cross-sections found that there were a few fibres, especially large fibres, that seemed have been ‘smeared’ during grinding and polishing. The ‘smeared’ fibres obviously created larger images and this effect would seem to cause an overestimation of fibre wall areas when these fibres are included in the measurements. The ‘smeared’ effect implies that the sample structure had not been supported sufficiently by the resin block. A possible reason for this could be that the resin that penetrated into the paper structure during degassing treatment was not replaced sufficiently by the mixture of the resin and the hardener in the subsequent step. Another possibility is that the resin and hardener mixture may not have penetrated into the fibre walls. This indicates that the sample surface is not free of artifacts although

great care has been taken during sample preparation. When measurements were taken $4\mu\text{m}$ below the sample surface, there were only a few large values (as shown in Figure 4-10 and Figure 4-11) and the measured mean values of fibre wall areas were close to the results obtained for the free fibres. It appears that any artifacts at the sample cross-sectional surface are eliminated by taking measurements at 4 microns below the sample cross-section. As mentioned before, the sample embedding technique was later improved by using a vacuum impregnation rig to allow the mixture of resin and hardener to penetrate the paper structure thoroughly. Figure 4-14 gives a group of paper cross-sectional images obtained from the sample embedded by the improved technique. As can be seen in Figure 4-14, the quality of images has been improved compare with those shown in Figure 4-5, and the ‘smeared’ effect cannot be seen in the image acquired at the sample surface. All of the later measurements were conducted in the $0\mu\text{m}$ images acquired by the improved technique.

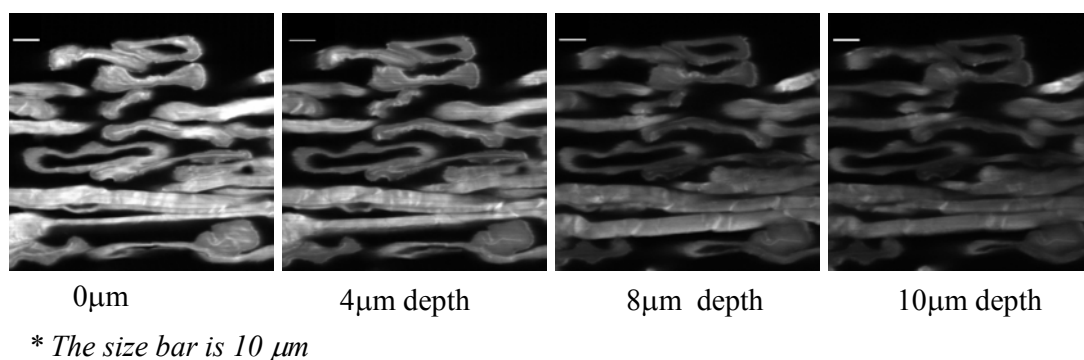


Figure 4-14 Cross-sectional images of paper acquired when the vacuum impregnation rig was used for sample embedding.

4.5.2 Comparison of the measured fibre orientation with the theoretical value

The average values of the angles of fibres to the X direction (Figure 4-5) are given in Table 4 1. The fibre orientation measured in this study was actually the orientation of fibre segments. In fact it is almost impossible to properly define the fibre orientation because fibres are not straight in a sheet. However, the orientation of fibre segments might be more important for paper properties than the average orientation of entire fibres.

In this study the measurement for fibre orientation calculation included any position shift of the fibre, in any direction, between the surface and 10µm depth into the paper cross-section. The fibres measured were sampled randomly through the whole thickness of the paper. Therefore, the fibre orientation measured is an overall fibre orientation. Although the position shift of fibres in sheets are not calculated in this chapter (such calculations will be shown in Chapter 6), in fact the positions of fibres were most likely to shift in both Y and Z directions (see Figure 4-5), although the shift in the Z direction was usually very small. If the position shift in the Z direction was zero, it indicates that the fibre is in-plane with respect to paper surface. Otherwise the fibre is out-of-plane. The small shift in the Z direction indicates that the out of plane movement of the fibres in the handsheets used in this study is small.

If θ is the in-plane fibre angle to any given line within the plane in the direction perpendicular to the exposed surface (the X direction in Figure 2), then from simple geometry the average value for a randomly oriented sheet, θ_{av} , is given by Equation 4.1. Integrating equation (1) gives an average value of $\pi/2-1$, or 32.7°.

$$\theta_{av} = \frac{\int_0^{\pi/2} \theta \cos \theta \, d\theta}{\int_0^{\pi/2} \cos \theta \, d\theta} \quad 4.1$$

From Table 4-1, there is about an 8° difference between the average measured value and this theoretical value of fibre orientation. This difference is considered to be reasonable because the theoretical value includes all fibres with angles between 0° and 90° but in this study fibres with high angles were excluded. After examining the raw data of fibre angles carefully, it was found that all the measured values seldom included fibres with angles over 80°. The reason for this is that the ‘high angle fibres’ are likely to be sectioned along the fibre axis and were treated as 90° fibres and not included in the measurements. This difference between the measured average fibre angle and the theoretical average value does not affect the validity of the angle measurements using the new technique. It appears that the effect of the out of plane movements of fibres in the sheets used in this study on the overall fibre orientation is negligible.

This study made no attempt at measuring the distribution of fibre orientation through the thickness of a sheet, however, the new technique could be used as needed to measure the distribution of fibre orientation through the thickness of a sheet.

4.6 Application of the New Technique

One possible application of the new technique is to quantify the behaviour of individual fibres in a sheet after wet pressing. Consolidation of the paper structure during pressing will occur through a combination of compressing fibres closer together and collapse of the fibres. How much the fibres are collapsed and brought closer together in wet pressing and how much these changes in individual fibres contribute to the densification of the sheet is still not clear. It is only possible to quantify these changes when the fibre dimensions in the sheet can be measured. The mechanisms of sheet densification will be studied in Chapter 6.

The new term, fibre fill factor, as defined in subsection 3.4.1 was used to quantify the collapse degree of fibres in sheets. As shown in Table 4-1, the fill factors of the recycled fibres in sheets show no significant change with increasing intensity of wet pressing. Additionally, the value of the fill factor measured in the 0 μ m depth images and that measured in the 4 μ m-depth images shows no significant difference. These results indicate that the collapse degree of the recycled fibres is not increased in wet pressing.

In the case of the kraft pulp fibres, the fill factor increases steadily as the pressing intensity is increased. This means that wet pressing has increased the degree of collapse of the kraft fibres in the sheets. The collapse behavior of the kraft fibres in wet pressing is different to that of the recycled fibres. A possible explanation for this difference is that the recycled fibres have already been collapsed to a certain degree during the previous papermaking process. It is therefore not easy to collapse these fibres further by wet pressing. The kraft pulp fibres were never dried and most of the fibres are uncollapsed. Therefore they are more likely to be collapsed in wet pressing.

The fibres in a sheet move closer together in wet pressing, forming more bonds. However other types of movement of fibres in wet pressing must still be clarified. One additional type of movement that was observed when the sheet was pressed was that the fibres were twisted so that they lay flat and became closer to each other. The new technique presented here can be used to quantify this twist of fibres in wet pressing. The twist angle defined in subsection 4.4.1.5 is used to quantifying the twist of fibres in wet pressing. The measured results of the twist angle will be discussed in Chapter 6.

Basing on the new technique, we have further developed a new technique for measuring fibre-fibre contacts in paper. The measured results will be outlined and discussed in Chapter 7.

4.7 Conclusions

Fibre dimensions, fibre orientation and fibre collapse have been measured directly in paper using a combined technique of resin embedding and confocal laser scanning microscopy. This is the first time a technique has been demonstrated for quantifying paper structure at the fibre level. Comparisons between the measured values of fibre wall areas by the new technique in paper with those measured by the routine confocal microscopy technique on free fibres show close agreement. The fibre orientation measured in the handsheets compares reasonably well with the theoretical value of fibre orientation of a random sheet. These results show that the measurements made by the new technique are valid.

Based on the new technique, new techniques for measuring fibre-fibre contacts have been developed. The new technique makes it possible to quantify the changes of individual fibres in paper in wet pressing and measure the fibre-fibre contacts directly in paper.